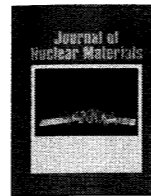




Contents lists available at SciVerse ScienceDirect

Journal of Nuclear Materials

journal homepage: www.elsevier.com/locate/jnucmat

Contents

Fifteenth International Conference on Fusion Reactor Materials

Preface: Fifteenth International Conference on Fusion Reactor Materials, R.E. Stoller, C.H. Henager and N.A. Uckan	S1	Effect of vanadium addition on the microstructure and mechanical properties of the ODS ferritic steels, Z. Oksiuta, M. Lewandowska, K.J. Kurzydowski and N. Baluc	S84
Reduced Activation Steels		Microstructure and high-temperature strength of high Cr ODS tempered martensitic steels, S. Ohtsuka, T. Kaito, T. Tanno, Y. Yano, S. Koyama and K. Tanaka	S89
Recent progress of R&D activities on reduced activation ferritic/martensitic steels, Q. Huang, N. Baluc, Y. Dai, S. Jitsukawa, A. Kimura, J. Konys, R.J. Kurtz, R. Lindau, T. Muroga, G.R. Odette, B. Raj, R.E. Stoller, L. Tan, H. Tanigawa, A.-A.F. Tavassoli, T. Yamamoto, F. Wan and Y. Wu	S2	Effects of titanium concentration and tungsten addition on the nano-mesoscopic structure of high-Cr oxide dispersion strengthened (ODS) ferritic steels, P. Dou, A. Kimura, R. Kasada, T. Okuda, M. Inoue, S. Ukai, S. Ohnuki, T. Fujisawa and F. Abe	S95
Effect of N on the precipitation behaviours of the reduced activation ferritic/martensitic steel CLF-1 after thermal ageing, P. Wang, J. Chen, H. Fu, S. Liu, X. Li and Z. Xu	S9	Influence of the low interfacial density energy on the coarsening resistivity of the nano-oxide particles in Ti-added ODS material, J. Ribis, M.-L. Lescoat, S.Y. Zhong, M.-H. Mathon and Y. de Carlan	S101
Effects of alloying elements and thermomechanical treatment on 9Cr Reduced Activation Ferritic–Martensitic (RAFM) steels, L. Tan, Y. Yang and J.T. Busby	S13	Incidence of mechanical alloying contamination on oxides and carbides formation in ODS ferritic steels, P. Olier, M. Couvrat, C. Cayron, N. Lochet and L. Charon	S106
Microsegregation in a F82H plate, H. Sakasegawa and H. Tanigawa	S18	Friction Consolidation of MA956 powder, D. Catalini, D. Kaoumi, A.P. Reynolds and G.J. Grant	S112
Nanoindentation hardness and its extrapolation to bulk-equivalent hardness of F82H steels after single- and dual-ion beam irradiation, Y. Takayama, R. Kasada, Y. Sakamoto, K. Yabuuchi, A. Kimura, M. Ando, D. Hamaguchi and H. Tanigawa	S23	Tensile and fracture characteristics of oxide dispersion strengthened Fe–12Cr produced by hot isostatic pressing, V. de Castro, J.M. Garcés-Usan, T. Leguey and R. Pareja	S119
Dependence of precipitate formation on normalizing temperature and its impact on the heat treatment of F82H-BA07 Steel, K. Fukumoto, T. Sakaguchi, K. Inoue, T. Itoh, H. Sakasegawa and H. Tanigawa	S28	Controlling the ductile to brittle transition in Fe–9%Cr ODS steels, S.F. Di Martino, N.B. Riddle and R.G. Faulkner	S124
Hydrogen traps in ion-irradiated F82H steel observed by NRA, I. Takagi, T. Komura, M. Akiyoshi, K. Moritani, T. Sasaki and H. Moriyama	S33	Charpy impact properties of 9CrODS ferritic steels, W. Izawa, S. Ukai, N. Oono, S. Hayashi, T. Sakamura, Y. Kohno, S. Ohtsuka and T. Kaito	S133
Application of master curve method to the evaluation of fracture toughness of F82H steels, B.J. Kim, R. Kasada, A. Kimura, E. Wakai and H. Tanigawa	S38	Strength correlation with residual ferrite fraction in 9CrODS ferritic steel, R. Miyata, S. Ukai, X. Wu, N. Oono, S. Hayashi, S. Ohtsuka and T. Kaito	S138
Effect of helium on fatigue crack growth and life of reduced activation ferritic/martensitic steel, S. Nogami, M. Takahashi, A. Hasegawa and M. Yamazaki	S43	Microstructure and tensile properties of oxide dispersion strengthened Fe–14Cr–0.3Y ₂ O ₃ and Fe–14Cr–2W–0.3Ti–0.3Y ₂ O ₃ , M.A. Auger, V. de Castro, T. Leguey, M.A. Monge, A. Muñoz and R. Pareja	S142
Characterization of helium ion implanted reduced activation ferritic/martensitic steel with positron annihilation and helium thermal desorption methods, I. Carvalho, H. Schut, A. Fedorov, N. Luzginova and J. Sietsma	S48	Microstructure of nano-structured ODS CLAM steel by mechanical alloying and hot isostatic pressing, C.-y. Lu, Z. Lu and C.-m. Liu	S148
Helium bubble morphology of boron alloyed EUROFER97 after neutron irradiation, M. Klimenkov, A. Möslang, E. Materna-Morris and H.-C. Schneider	S52	Tensile properties and microstructure of helium implanted EUROFER ODS, A.I. Ryazanov, O.K. Chugunov, S.M. Ivanov, S.T. Latushkin, R. Lindau, A. Möslang, A.A. Nikitina, K.E. Prikhodko, E.V. Semenov, V.N. Unezhev and P.V. Vladimirov	S153
Fracture toughness characterization in the lower transition of neutron irradiated Eurofer97 steel, N. Ilchuk, P. Spätig and G.R. Odette	S58	Structure of complex oxide nanoparticles in a Fe–14Cr–2W–0.3Ti–0.3Y ₂ O ₃ ODS RAF steel, P. Unifantowicz, T. Płociński, C.A. Williams, R. Schäublin and N. Baluc	S158
Tensile and low cycle fatigue properties of EUROFER97-steel after 16.3 dpa neutron irradiation at 523, 623 and 723 K, E. Materna-Morris, A. Möslang and H.-C. Schneider	S62	Morphology of oxide particles in ODS austenitic stainless steel, H. Oka, M. Watanabe, N. Hashimoto, S. Ohnuki, S. Yamashita and S. Ohtsuka	S164
Continuous cooling transformation behaviors of CLAM steel, Q.-s. Wu, S.-h. Zheng, Q.-y. Huang, S.-j. Liu and Y.-y. Han	S67	Development of 15CrODS ferritic steels for over 1273 K service, Y. Sawazaki, S. Ukai, Y. Sugino, S. Hayashi, N. Oono, K. Hamajima and A. Niwa	S169
Mechanical properties and microstructure evolution of CLAM Steel in tube fabrication and test blanket module assembly, B. Huang, Q. Huang, Y. Li, C. Li, Q. Wu and FDS Team	S71		
ODS/Advanced Steels		Plasma Facing Materials	
IAEA coordinated research activities on materials for advanced reactor systems, A. Zeman, V. Inozemtsev, R. Kamendje and R.L. Beatty	S77	A brief summary of the progress on the EFDA tungsten materials program, M. Rieth, S.L. Dudarev, S.M. Gonzalez de Vicente, J. Aktaa, T. Ahlgren, S. Antusch, D.E.J. Armstrong, M. Balden, N. Baluc, M.-F. Barthe, W.W. Basuki, M. Battabyal, C.S. Becquart, D. Blagoeva, H. Boldyryeva, J. Brinkmann, M. Celino, L. Ciupinski, J.B. Correia, A. De Backer, C. Domain, E. Gaganidze, C. Garcia-Rosales, J. Gibson, M.R. Gilbert, S. Giusepponi, B. Gludovatz, H. Greuner, K. Heinola, T. Höschen, A. Homann, N. Holstein, F. Koch, W. Krauss, H. Li, S. Lindig, J. Linke, Ch. Linsmeier, P. Lopez-Ruiz, H. Maier, J. Matejcek, T.P. Mishra, M. Muhammed, A. Munoz, M. Muzyk, K. Nordlund, D. Nguyen-Manh, J. Opschoor, N. Ordas, T. Palacios, G. Pintsuk, R. Pippin, J. Reiser, J. Riesch, S.G. Roberts, L. Romaner, M. Rosiński, M. Sanchez, W. Schulmeyer, H. Traxler, A. Urena, J.G. van der Laan, L. Veleva, S. Wahlberg, M. Walter, T. Weber, T. Weitkamp, S. Wurster, M.A. Yar, J.H. You and A. Zivelonghi	S173
		Recent progress in R&D on tungsten alloys for divertor structural and plasma facing materials, S. Wurster, N. Baluc, M. Battabyal, T. Crosby, J. Du, C. Garcia-Rosales, A. Hasegawa, A. Homann, A. Kimura, H. Kurishita, R.J. Kurtz, H. Li, S. Noh, J. Reiser, J. Riesch, M. Rieth, W. Setyawan, M. Walter, J.-H. You and R. Pippin	S181
		Status of R&D on plasma facing materials in China, Q.-Z. Yan, X.-F. Zhang, Z.-J. Zhou, W.-P. Shen, Y.-C. Zhang, S.-M. Wang, L. Xu and C.-c. Ge	S190
		Development of tungsten and tungsten alloys for DEMO divertor applications via MIM technology, D.T. Blagoeva, J. Opschoor, J.G. van der Laan, C. Sârbu, G. Pintsuk, M. Jong, T. Bakker, P. Ten Pierick and H. Nolles	S198
		Charpy impact properties of pure tungsten plate material in as-received and recrystallized condition (1 h at 2000 °C (2273 K)), J. Reiser, M. Rieth, B. Daerner and A. Homann	S204
		Preparation of W–Cu functionally graded material coated with CVD–W for plasma-facing components, J. Song, Y. Yu, Z. Zhuang, Y. Lian, X. Liu and Y. Qi	S208
		Influence of processing route and yttria additions on the oxidation behavior of tungsten, S.C. Cifuentes, A. Muñoz, M.A. Monge and P. Pérez	S214
		Powder metallurgical processing of self-passivating tungsten alloys for fusion first wall application, P. López-Ruiz, N. Ordás, I. Iturriza, M. Walter, E. Gaganidze, S. Lindig, F. Koch and C. Garcia-Rosales	S219
		Microstructure and mechanical properties of a W–2wt.%Y ₂ O ₃ composite produced by sintering and hot forging, M. Battabyal, R. Schäublin, P. Spätig, M. Walter, M. Rieth and N. Baluc	S225
		Microstructure and temperature dependence of the microhardness of W–4V–1La ₂ O ₃ and W–4Ti–1La ₂ O ₃ , B. Savoini, J. Martinez, A. Muñoz, M.A. Monge and R. Pareja	S229
		Effect of hot working process on the mechanical properties of tungsten materials, Q. Yan, X. Zhang, T. Wang, C. Yang and C. Ge	S233
		Erosion of tungsten and its brazed joints with bronze irradiated by pulsed deuterium plasma flows, V. Yakushin, V. Polsky, B. Kalin, P. Dzhumayev, A. Polyansky, O. Sevryukov, A. Suchkov and V. Fedotov	S237
		Behavior of deuterium retention and surface morphology for VPS–W/F82H, Y. Oya, M. Shimada, T. Tokunaga, A. Kimura and K. Okuno	S242
		In situ observation of deuterium trapping in self-ion irradiated tungsten, I. Takagi, K. Yamamichi, Y. Furuta, M. Akiyoshi, T. Sasaki, H. Tsuchida and Y. Hatano	S246
		Effects of helium and deuterium irradiation on SPS sintered W–Ta composites at different temperatures, R. Mateus, M. Dias, J. Lopes, J. Rocha, N. Catarino, N. Franco, V. Livramento, P.A. Carvalho, J.B. Correia, K. Hanada and E. Alves	S251
		Investigation of European tungsten materials exposed to high heat flux H/He neutral beams, H. Greuner, H. Maier, M. Balden, Ch. Linsmeier, B. Bösowirth, S. Lindig, P. Norajitra, S. Antusch and M. Rieth	S256
		Multiphysics model of thermomechanical and helium-induced damage of tungsten during plasma heat transients, T. Crosby and N.M. Ghoniem	S261
		Helium effects on tungsten surface morphology and deuterium retention, Y. Ueda, H.Y. Peng, H.T. Lee, N. Ohno, S. Kajita, N. Yoshida, R. Doerner, G. De Temmerman, V. Alimov and G. Wright	S267
		Property change of advanced tungsten alloys due to neutron irradiation, M. Fukuda, A. Hasegawa, T. Tanno, S. Nogami and H. Kurishita	S273
		Mechanical behavior of tungsten–vanadium–lanthana alloys as function of temperature, T. Palacios, J.Y. Pastor, M.V. Aguirre, A. Martín, M.A. Monge, A. Muñoz and R. Pareja	S277
		Thermal shock behavior of tungsten based alloys manufactured via powder injection molding, G. Pintsuk, D. Blagoeva and J. Opschoor	S282
		Development of high-grade VPS-tungsten coatings on F82H reduced activation steel, T. Tokunaga, H. Watanabe, N. Yoshida, T. Nagasaka, R. Kasada, Y.-J. Lee, A. Kimura, M. Tokitani, M. Mitsuhashi, T. Hinoki, H. Nakashima, S. Masuzaki, T. Takabatake, N. Kuroki, K. Ezato, S. Suzuki and M. Akiba	S287
		Investigation on the microstructure of W-coated low-activation alloy V–4Cr–4Ti, H. Watanabe, T. Tokunaga, N. Yoshida, T. Nagasaka and T. Muroga	S292
		High heat load properties of nanostructured, recrystallized W–1.1TiC, K. Tokunaga, H. Kurishita, H. Arakawa, S. Matsuo, T. Hotta, K. Araki, Y. Miyamoto, T. Fujiwara, K. Nakamura, T. Takida, M. Kato and A. Ikegaya	S297
		Development of micro-engineered textured tungsten surfaces for high heat flux applications, S. Sharafat, A. Aoyama, B. Williams and N. Ghoniem	S302
		Vacuum hot-pressed beryllium and TiC dispersion strengthened tungsten alloy developments for ITER and future fusion reactors, X. Liu, J. Chen, Y. Lian, J. Wu, Z. Xu, N. Zhang, Q. Wang, X. Duan, Z. Wang and J. Zhong	S309
		Properties of deposited layer formed by interaction with Be seeded D–He mixture plasma and tungsten, K. Tokunaga, M.J. Baldwin, D. Nishijima, R.P. Doerner, S. Nagata, B. Tsuchiya, H. Kurishita, T. Fujiwara, K. Araki, Y. Miyamoto, N. Ohno and Y. Ueda	S313
		Formation and delamination of beryllium carbide films, R. Mateus, P.A. Carvalho, N. Franco, L.C. Alves, M. Fonseca, C. Porosnicu, C.P. Lungu and E. Alves	S320
		Vanadium Alloys	
		Assessment of a European V–4Cr–4Ti alloy – CEA-J57, M. Le Flem, J.-M. Gentzbittel and P. Wident	S325
		Investigation on mechanical alloying process for vanadium alloys, P.F. Zheng, T. Nagasaka, T. Muroga and J.M. Chen	S330
		Fabrication using electron beam melting of a V–4Cr–4Ti alloy and its thermo-mechanical strengthening study, H.Y. Fu, J.M. Chen, P.F. Zheng, T. Nagasaka, T. Muroga, Z.D. Li, S. Cui and Z.Y. Xu	S336
		Effect of yttrium on dynamic strain aging of vanadium alloys, T. Miyazawa, T. Nagasaka, Y. Hishinuma, T. Muroga, Y. Li, Y. Satoh, S. Kim and H. Abe	S341
		Irradiation-induced precipitation in V–4Cr–4Ti alloys studied using three-dimensional atom probe, M. Hatakeyama, T. Nagasaka, T. Muroga, T. Toyama and I. Yamagata	S346
		Tensile testing study of dynamic interactions between dislocations and precipitate in vanadium alloys, K. Tougo, K. Nogiwa, K. Tachikawa and K.-i. Fukumoto	S350
		Dislocation evolution during thermal creep deformation in V–4Cr–4Ti with various thermal and mechanical treatments, T. Muroga, T. Nagasaka, P.F. Zheng, Y.F. Li and H. Watanabe	S354
		Recovery process of neutron-irradiated vanadium alloys in post-irradiation annealing treatment, K. Fukumoto, M. Iwasaki and Q. Xu	S360
		Impact property of low-activation vanadium alloy after laser welding and heavy neutron irradiation, T. Nagasaka, T. Muroga, H. Watanabe, T. Miyazawa, M. Yamazaki and K. Shinozaki	S364
		SiC, SiC-Fibers, and SiC-Composites	
		Transmutation of silicon carbide in fusion nuclear environment, M.E. Sawan, Y. Katoh and L.L. Snead	S370
		Thermo-physical, -mechanical, and -electrical behaviors of ion-irradiated Tyranno-SA SiC fibers at high temperatures (1473 K), K. Shimoda and C. Colin	S376
		Effect of differential swelling between fiber and matrix on the strength of irradiated SiC/SiC composites, T. Koyanagi, S. Kondo and T. Hinoki	S380
		Effect of thermal cycling of SiC/SiC composites on their mechanical properties, A. Udayakumar, M. Stalin, M.B. Abhayalakshmi, R. Hariharan and M. Balasubramanian	S384

Characterization of slurry infiltrated SiC _f /SiC prepared by electro-phoretic deposition, <i>J.Y. Park, M.H. Jeong and W.-J. Kim</i>	S390
Effects of neutron irradiation on polymorphs of silicon nitride and SiAlON ceramics, <i>A. Rueanngoen, K. Kanazawa, M. Akiyoshi, M. Imai, K. Yoshida and T. Yano</i>	S394
Recovery behavior of point defects after low-dose neutron irradiation at ~423 K of sintered 6H-SiC by lattice parameter and macroscopic length measurements, <i>T. Yano, Y. Futamura, S. Yamazaki, T. Sawabe and K. Yoshida</i>	S399
Radioluminescence characterization of SiC and SiC/SiC for 1.8 MeV electron irradiation, <i>M. Malo, A. Morono and E.R. Hodgson</i>	S404
Effects of contact resistance on electrical conductivity measurements of SiC-based materials, <i>G.E. Youngblood, E.C. Thomsen and C.H. Henager Jr.</i>	S410

Breeder Blanket Materials

Assessment of materials data for blanket materials within the European contribution to ITER, <i>S. Wikman, A. Peacock, O. Zlamal, J. Öjjerholm, S. Tähtinen, M. Rödig, P. Marmy, O. Gillia, P. Lorenzetto and S. Heikkinen</i>	S414
Recent developments of solid breeder fabrication, <i>R. Knitter, P. Chaudhuri, Y.J. Feng, T. Hoshino and I.-K. Yu</i>	S420
Development of methods for reprocessing and reuse of tritium breeder materials in broader approach activities, <i>T. Hoshino</i>	S425
Effects of threshold displacement energy on defect production by displacement cascades in α , β and γ -LiAlO ₂ , <i>H. Tsuchihira, T. Oda and S. Tanaka</i>	S429
Fabrication of modified lithium orthosilicate pebbles by addition of titania, <i>R. Knitter, M.H.H. Kolb, U. Kaufmann and A.A. Goraieb</i>	S433
Release behavior of hydrogen isotopes thermally sorbed in Li ₂ TiO ₃ single crystal, <i>D. Zhu, T. Oda, Y. Shono and S. Tanaka</i>	S437
Composition change of the near-surface layer of Li ₂ TiO ₃ after CO ₂ absorption observed with accelerator analyses, <i>Y. Furuyama, Y. Sasaki, Y. Gotoh, A. Taniike and A. Kitamura</i>	S442
Vaporization property and crystal structure of lithium metatitanate with excess Li, <i>K. Mukai, K. Sasaki, T. Terai, A. Suzuki and T. Hoshino</i>	S447
Radiation enhanced diffusion and redistribution of helium in LiNbO ₃ , <i>A. Morono and E.R. Hodgson</i>	S451
Effect of cation exchange on hydrogen adsorption property of mor-denite for isotope separation, <i>Y. Kawamura, Y. Iwai, K. Munakata and T. Yamaniishi</i>	S455
The effect of sintering time on synthesis of plasma sintered beryllides, <i>J.-H. Kim and M. Nakamichi</i>	S461
Preliminary characterization of plasma-sintered beryllides as advanced neutron multipliers, <i>M. Nakamichi, J.H. Kim, K. Munakata, T. Shibayama and M. Miyamoto</i>	S465
Analysis of tritium retention in beryllium pebbles in EXOTIC, PBA and HIDOBE-01 experiments, <i>A.V. Fedorov, S. van Til, L.J. Magielsen and M.P. Stijkel</i>	S472
Tritium release from beryllium pebbles after high temperature irradiation up to 3000 appm He in the HIDOBE-01 experiment, <i>S. van Til, A.V. Fedorov, M.P. Stijkel, H.L. Cobussen, R.K. Mutnuru, P. v.d. Idsert and M. Zmitko</i>	S478
Tritium release and retention properties of highly neutron-irradiated beryllium pebbles from HIDOBE-01 experiment, <i>V. Chakin, R. Rolli, A. Moeslang, M. Klimenkov, M. Kolb, P. Vladimirov, P. Kurinskiy, H.-C. Schneider, S. van Til, A.J. Magielsen and M. Zmitko</i>	S483
Tritium release behavior of beryllium pebbles after neutron irradiation between 523 and 823 K, <i>A. Vitiņš, G. Ķizāne, A. Matīss, E. Pajuste and V. Zubkovs</i>	S490
Oxidation resistance of Be ₁₂ Ti fabricated by plasma-sintering method, <i>K. Wada, K. Munakata, J.H. Kim, K. Yonehara, D. Wakai and M. Nakamichi</i>	S494
Tritium trapping in silicon carbide in contact with solid breeder under high flux isotope reactor irradiation, <i>H. Katsui, Y. Katoh, A. Hasegawa, M. Shimada, Y. Hatano, T. Hinoki, S. Nogami, T. Tanaka, S. Nagata and T. Shikama</i>	S497

Diagnostic Materials

Recent research activities on functional ceramics for insulator, breeder and optical sensing systems in fusion reactors, <i>S. Nagata, H. Katsui, K. Hoshi, B. Tsuchiya, K. Toh, M. Zhao, T. Shikama and E.R. Hodgson</i>	S501
Neutron irradiation of modern KU-1 and KS-4V fused silica, <i>I.I. Orlovskiy, K.Yu. Vukolov, E.N. Andreenko and T.R. Mukhammedzyanov</i>	S508
Observation of radiation damage in silica glass using ion-induced luminescence, <i>K. Furumoto and T. Tanabe</i>	S511
Low-energy helium irradiation on in-vessel mirror materials, <i>S. Kajita, M. Tokitani, T. Saeki, N. Ohno and N. Yoshida</i>	S515
Radioluminescence monitoring of radiation induced surface electrical degradation in aluminas, <i>M. Malo, A. Morono and E.R. Hodgson</i>	S520

Joining, Bonding, and Welding

Mechanical properties of friction stir welded 11Cr-ferritic/martensitic steel, <i>Y. Yano, Y.S. Sato, Y. Sekio, S. Ohtsuka, T. Kaito, R. Ogawa and H. Kokawa</i>	S524
Joining of 14YWT and F82H by friction stir welding, <i>D.T. Hoelzer, K.A. Unocic, M.A. Sokolov and Z. Feng</i>	S529
Numerical study of local PWHT condition for EB welded joint between first and side walls in ITER-TBM, <i>H. Serizawa, S. Nakamura, H. Tanigawa, H. Ogiwara and H. Murakawa</i>	S535
Joining of tungsten to ferritic/martensitic steels by hot isostatic pressing, <i>J.-Y. Park, Y.-I. Jung, B.-K. Choi, D.-W. Lee and S. Cho</i>	S541
Oxide formation and precipitation behaviors on interface of F82H steel joints during HIPing and hot pressing, <i>H. Kishimoto, T. Ono, H. Sakasegawa, H. Tanigawa, M. Ando, T. Shibayama, Y. Kohno and A. Kohyama</i>	S546
Characterization of ODS (Oxide Dispersion Strengthened) Eurofer/Eurofer dissimilar electron beam welds, <i>L. Commin, M. Rieth, V. Widak, B. Daerner, S. Heger, H. Zimmermann, E. Materna-Morris and R. Lindau</i>	S552
Irradiation response in weldment and HIP joint of reduced activation ferritic/martensitic steel, F82H, <i>T. Hirose, M.A. Sokolov, M. Ando, H. Tanigawa, K. Shiba, R.E. Stoller and G.R. Odette</i>	S557
Study on electron beam weld joints between pure vanadium and SUS316L stainless steel, <i>S. Nogami, J. Miyazaki, A. Hasegawa, T. Nagasaka and T. Muroga</i>	S562
Grain refinement of transient liquid phase bonding zone using ODS insert foil, <i>H. Noto, R. Kasada, A. Kimura and S. Ukai</i>	S567

Corrosion Science and Coatings

Pb–Li compatibility issues for DEMO, <i>B.A. Pint and K.A. Unocic</i>	S572
Corrosion and precipitation effects in a forced-convection Pb–15.7Li loop, <i>J. Konys and W. Krauss</i>	S576
Characterization of specimens exposed in a Li loop, <i>K.A. Unocic, M.J. Lance and B.A. Pint</i>	S580
Electrodeposition of metallic tungsten coating from binary oxide molten salt on low activation steel substrate, <i>Y.H. Liu, Y.C. Zhang, F. Jiang, B.J. Fu and N.B. Sun</i>	S585
Fabrication and deuterium permeation properties of erbia-metal multilayer coatings, <i>T. Chikada, A. Suzuki, F. Koch, H. Maier, T. Terai and T. Muroga</i>	S592
Preliminary study of HDA coating on CLAM steel followed by high temperature oxidation, <i>X. Chen, Q. Huang, Z. Yan, Y. Song, S. Liu and Z. Jiang</i>	S597
Characterization of the alumina film with cerium doped on the iron-aluminide diffusion coating, <i>Q. Zhan, H.G. Yang, W.W. Zhao, X.M. Yuan, Y. Hu, and TMT Team</i>	S603

Fundamental Modeling

Continuum modeling of plastic flow localization in irradiated fcc metals, <i>G. Po and N. Ghoniem</i>	S607
The effects of temperature on (001)⟨110⟩ crack propagation in bcc iron, <i>V.A. Borodin, P.V. Vladimirov and A. Möslang</i>	S612
MD simulation of atomic displacement cascades near chromium-rich clusters in FeCr alloy, <i>M. Tikhonchev, V. Svetukhin and E. Gaganidze</i>	S618
Modeling of chromium nanocluster growth under neutron irradiation, <i>V. Svetukhin, P. Lvov, M. Tikhonchev, E. Gaganidze and N. Krestina</i>	S624
Interaction of dislocations with Frank loops in Fe–Ni alloys and pure Ni: An MD study, <i>D. Terentyev, A. Bakaev and Yu.N. Osetsky</i>	S628
Effect of anisotropy, SIA orientation, and one-dimensional migration mechanisms on dislocation bias calculations in metals, <i>D. Seif and N.M. Ghoniem</i>	S633
KMC clustering model comparison in BCC iron, <i>A. Oaks and J.F. Stubbins</i>	S639
Molecular dynamics study of strengthening by nanometric void and Cr alloying in Fe, <i>R. Schäublin and S.M. Hafez Haghighat</i>	S643
Quantifying He-point defect interactions in Fe through coordinated experimental and modeling studies of He-ion implanted single-crystal Fe, <i>X. Hu, D. Xu and B.D. Wirth</i>	S649
An atomistic modeling of He bubble stability at grain boundaries in alpha-Fe, <i>T. Suzudo, T. Tsuru, M. Yamaguchi and H. Kaburaki</i>	S655
Interstitial helium diffusion mechanisms in (110) tilt grain boundaries in BCC FeCr alloys: A atomistic study, <i>X. He, D. Terentyev, Y. Lin and W. Yang</i>	S660
Diffusion of small He clusters in bulk and grain boundaries in α -Fe, <i>H.Q. Deng, W.Y. Hu, F. Gao, H.L. Heinisch, S.Y. Hu, Y.L. Li and R.J. Kurtz</i>	S667
Molecular dynamics simulation of cascade-induced ballistic helium resolutioning from bubbles in iron, <i>R.E. Stoller</i>	S674
First-principles model for phase stability, radiation defects and elastic properties Of W–Ta and W–V alloys, <i>M. Muzyk, D. Nguyen-Manh, J. Wróbel, K.J. Kurzydłowski, N.L. Baluc and S.L. Dudarev</i>	S680
First-principles thermodynamic calculations of diffusion characteristics of impurities in γ -iron, <i>T. Tsuru and Y. Kaji</i>	S684
First-principles investigation on vacancy trapping behaviors of hydrogen in vanadium, <i>L.-J. Gui, Y.-L. Liu, W.-T. Wang, S. Jin, Y. Zhang, G.-H. Lu and J.-E. Yao</i>	S688
Ab initio static and molecular dynamics studies of helium behavior in beryllium, <i>P.V. Vladimirov and A. Moeslang</i>	S694
Calculation of damage function of Al ₂ O ₃ in irradiation facilities for fusion reactor applications, <i>F. Mota, C.J. Ortiz, R. Vila, N. Casal, A. Garcia and A. Ibarra</i>	S699
First-principles calculations for the surface termination of Li ₂ TiO ₃ (001) surfaces, <i>K. Azuma, T. Oda and S. Tanaka</i>	S705

Hydrogen and Helium Effects and Tritium Permeation

The role of radiation damage on retention and temperature intervals of helium and hydrogen detrapping in structural materials, <i>G.D. Tolstoluskaya, V.V. Ruzhytskyi, V.N. Voyevodin, I.E. Kopanets, S.A. Karpov and A.V. Nikitin</i>	S710
Helium irradiation effects on deuterium retention in tungsten, <i>Y. Sakoi, M. Miyamoto, K. Ono and M. Sakamoto</i>	S715
Influence of the Cr content on the permeation of hydrogen in Fe alloys, <i>I. Peñalva, G. Alberro, J. Aranburu, F. Legarda, J. Sancho, R. Vila and C.J. Ortiz</i>	S719
Tritium permeation and desorption in reduced activation martensitic steels studied in EXOTIC-9/1 irradiation experiment, <i>A.V. Fedorov, S. van Til, A.J. Magielsen and M.P. Stijkel</i>	S723
Hydrogen permeation in iron and nickel alloys around room temperature, <i>T. Otsuka, M. Shinohara, H. Horinouchi and T. Tanabe</i>	S726
Fatigue behavior of He-pre-injected 316 stainless steel under 17 MeV proton irradiation, <i>Y. Murase and N. Yamamoto</i>	S730
Effects of hydrogen on interaction between dislocations and radiation-induced defects in austenitic stainless steels, <i>T. Miura, K. Fujii, H. Nishioka and K. Fukuya</i>	S735

Tritium migration in the materials proposed for fusion reactors: Li ₂ TiO ₃ and beryllium, <i>T.V. Kulsartov, Yu.N. Gordienko, I.L. Tazhibayeva, E.A. Kenzhin, N.I. Barsukov, A.O. Sadvakasova, A.V. Kulsartova and Zh.A. Zaurbekova</i>	S740
Desorption of hydrogen trapped in carbon and graphite, <i>H. Atsumi, Y. Takemura, T. Miyabe, T. Konishi, T. Tanabe and T. Shikama</i>	S746
Recombination of atomic oxygen and hydrogen on amorphous carbon, <i>A. Drenik, A. Vesel, M. Mozetič and P. Panjan</i>	S751

Microstructure Evolution

Neutron-induced dpa, transmutations, gas production, and helium embrittlement of fusion materials, <i>M.R. Gilbert, S.L. Dudarev, D. Nguyen-Manh, S. Zheng, L.W. Packer and J.-Ch. Sublet</i>	S755
On the formation of stacking fault tetrahedra in irradiated austenitic stainless steels – A literature review, <i>R. Schibli and R. Schäublin</i>	S761
Defect clusters formed from large collision cascades in fcc metals irradiated with spallation neutrons, <i>Y. Satoh, Y. Matsuda, T. Yoshiie, M. Kawai, H. Matsumura, H. Iwase, H. Abe, S.W. Kim and T. Matsunaga</i>	S768
Damage rate dependence of defect cluster nucleation in tungsten during irradiation, <i>Y. Yamamoto, J. Yoshimatsu and K. Morishita</i>	S773
Effect of stress on radiation-induced hardening of A533B and Fe–Mn model alloys, <i>H. Watanabe, A. Hiragane, S. Shin, N. Yoshida and Y. Kamada</i>	S776
The effect of C concentration on radiation damage in Fe–Cr–C alloys, <i>A. Meinander, K.O.E. Henriksson, C. Björkas, K. Vörtler and K. Nordlund</i>	S782
Comparison between bulk and thin foil ion irradiation of ultra high purity Fe, <i>A. Prokhodtseva, B. Décamps and R. Schäublin</i>	S786
Effect of alloying elements on irradiation hardening behavior and microstructure evolution in BCC Fe, <i>K. Yabuuchi, R. Kasada and A. Kimura</i>	S790
Analysis of helium and hydrogen effect on RAJS by means of multi-beam electron microscope, <i>N. Hashimoto, J. Tanimoto, T. Kubota, H. Kinoshita and S. Ohnuki</i>	S796
Microstructural evolution in proton irradiated NF616 at 773 K to 3 dpa, <i>Y. Huang, J.P. Wharry, Z. Jiao, C.M. Parish, S. Ukai and T.R. Allen</i>	S800
Microstructure of Ni fatigued under neutron irradiation, <i>K. Sato, X.Z. Cao, T. Yoshiie, Q. Xu, C. Kutsukake and C. Konno</i>	S805
Microstructure and swelling of neutron irradiated nickel and binary nickel alloys, <i>S.I. Porollo, A.M. Dvoriashin, Yu.V. Konobeev and F.A. Garner</i>	S809
Effects of alloying elements on defect structures in the incubation period for void swelling in austenitic stainless steels, <i>M. Horiki, T. Yoshiie, S.S. Huang, K. Sato, X.Z. Cao, Q. Xu and T.D. Troev</i>	S813
Synergistic effects of helium and hydrogen on self-ion-induced swelling of austenitic 18Cr10NiTi stainless steel, <i>O.V. Borodin, V.V. Bryk, A.S. Kalchenko, V.V. Melnichenko, V.N. Voyevodin and F.A. Garner</i>	S817
A comparative TEM study of in-reactor and post-irradiation tensile tested copper, <i>J. Pakarinen, S. Tähtinen and B.N. Singh</i>	S821
Comparison of irradiation hardening and microstructure evolution in ion-irradiated delta and epsilon hydrides, <i>N. Oono, R. Kasada, T. Higuchi, K. Sakamoto, M. Nakatsuka, A. Hasegawa, S. Kondo, N.Y. Iwata, H. Matsui and A. Kimura</i>	S826
Stability of precipitates in ZIRLO under high energy particle irradiation, <i>H. Hayashi, N. Hashimoto and S. Ohnuki</i>	S830

Characterization Tools and Techniques

Advanced materials characterization and modeling using synchrotron, neutron, TEM, and novel micro-mechanical techniques—A European effort to accelerate fusion materials development, <i>Ch. Linsmeier, C.-C. Fu, A. Kaprolat, S.F. Nielsen, K. Mergia, R. Schäublin, R. Lindau, H. Bolt, J.-Y. Buffière, M.J. Caturla, B. Décamps, C. Ferrero, H. Greuner, C. Hébert, T. Höschen, M. Hofmann, C. Hugenschmidt, T. Jourdan, M. Köppen, T. Płociński, J. Riesch, M. Scheel, B. Schillinger, A. Vollmer, T. Weitkamp, W. Yao, J.-H. You, A. Zivelonghi, and the FEMaS-CA partners</i>	S834
---	------

Irradiation-induced precipitation in a SUS316 stainless steel using three-dimensional atom probe, <i>M. Hatakeyama and I. Yamagata</i>	S846	A new high-temperature indentation device for characterization of materials for fusion applications, <i>B. Albinski, H.-C. Schneider, I. Sacksteder and O. Kraft</i>	S865
Observation of interaction behavior between microstructural defects and dislocation by in situ strain TEM examination, <i>H.-H. Jin, C. Shin and J. Kwon</i>	S851	On determination of the constitutive behavior of tempered martensitic steels from micro-indentations: Application to Eurofer97 steel, <i>P. Spätig and N. Ilchuk</i>	S869
Radiation damage in nanocrystalline Ni under irradiation studied using positron annihilation spectroscopy, <i>H. Tsuchida, T. Iwai, M. Awano, N. Oshima, R. Suzuki, K. Yasuda, C. Batchuluun and A. Itoh</i>	S856	Evaluation of the surface morphologies and erosion/deposition profiles on the LHD first-wall by using toroidal array probes, <i>M. Tokitani, S. Masuzaki, N. Yoshida, T. Akiyama, N. Noda, A. Sagara, H. Yamada, T. Muroga, S. Nagata and B. Tsuchiya</i>	S873
Ion-irradiation enhancement of materials degradation in Fe–Cr single crystals detected by magnetic technique, <i>Y. Kamada, H. Watanabe, S. Mitani, J.N. Mohapatra, H. Kikuchi, S. Kobayashi, M. Mizuguchi and K. Takanashi</i>	S861	Study on kinetics of hydrogen dissolution and hydrogen solubility in oxides using imaging plate technique, <i>K. Hashizume, K. Ogata, M. Nishikawa, T. Tanabe, S. Abe, S. Akamaru and Y. Hatano</i>	S880